Donating Strength of Azulene in Various Azulen-1-yl-Substituted Cationic Dyes: Application in Nonlinear Optics

Liliana Cristian,† Isabelle Sasaki, Pascal G. Lacroix,* and Bruno Donnadieu

Laboratoire de Chimie de Coordination du CNRS, 205 route de Narbonne, 31077 Toulouse, France

Inge Asselberghs and Koen Clays

Laboratorium voor Chemische en Biologische Dynamica, Katholieke Universiteit Leuwen, Celestijnenlaan 200D, B-3001 Leuwen, Belgium

Alexandru C. Razus

C.D. Nentzescu Institute of Organic Chemistry, POX 258, 71141 Bucharest 15, Romania

Received May 3, 2004. Revised Manuscript Received June 25, 2004

Three new azulene-based substituted pyridinium cations, azulene-1-azo(*N*-methyl-4′-pyridinium) (**1**$^+$), azulene-1-[(*E*)-2-(*N*-methyl-4′-pyridinium)ethenyl] (**2**$^+$), and azulene-1-azo-[(*N*-methyl-5′-quinolinium)] (**3**$^+$) were synthesized, and their crystal structures solved by X-ray diffraction. A set of crystallographic, spectroscopic, and computational investigations reveals that, while the pyridinium is a very strong acceptor unit, the azulene counterpart acts as an extremely efficient electron donor in these chromophores. The static quadratic hyperpolarizabilities (β_0), measured by the hyper Rayleigh scattering method, are equal to 67×10^{-30}, 108×10^{-30}, and 80×10^{-30} cm^5 esu^{-1}, for **1**$^+$, **2**$^+$, and **3**$^+$, respectively. Interestingly, these values are slightly reduced versus those recorded on the related stilbazolium derivatives built up from the less efficient (dimethylamino)phenyl donor substituent. This observation suggests that the donor strength of azulene is beyond the point which maximizes β in the "push−pull" (arylethenyl)pyridinium series. An important charge delocalization in the ground state is suggested to account for the reduced β value in these chromophores, in agreement with the calculated charge-transfer properties, Mulliken charges, and experimental solvatochromism. These investigations suggest that azulene could attract an additional interest in the design of chromophores with cubic optical nonlinearities.

Introduction

Organic molecules with large nonlinear optical (NLO) responses have the potential to supplant the ferroelectric crystals commercially available (e.g., $LiNbO_3$ or KH_2PO_4),[1] by virtue of their large quadratic (β) and cubic (γ) molecular hyperpolarizabilities, in addition to an ultrafast response time and large damage threshold.[2] The development of these materials has certainly been deeply boosted by the tremendous capabilities of organic synthesis. After the substituted stilbene series, which was the benchmark family of NLO chromophores throughout the 1980s,[3] alternative structures have more recently been under investigation, such as one-dimensional arylethynyl porphyrins[4] and polyenes.[5] Molecules with higher dimensionality have also been explored for their off-diagonal contribution to the NLO response. These efforts have been stimulated by the emergence of the intriguing concept of octupolar geometries (e.g., T_d, D_{3h}, and D_{2d}),[6] but two-dimensional charge-transfer molecules (e.g., C_2 geometry) have also provided NLO candidates with enhanced capabilities in some cases.[7] Alternatively, computational approaches have been proposed, which consist in starting from known efficient

* To whom correspondence should be addressed.

† Permanent address: C.D. Nentzescu Institute of Organic Chemistry, POX 258, 71141 Bucharest 15, Romania.

(1) Kurtz, S. K. In *Nonlinear Optical Materials—Laser Handbook*; Arecchi F. T., Schultz-Dubois E. O., Eds.; North-Holland: Amsterdam, 1972; Vol. 1, p 923.

(2) (a) *Molecular Nonlinear Optics: Materials, Physics, and Devices*; Zyss, J., Ed.; Academic Press: New York, 1994. (b) *Nonlinear Optics of Organic Molecules and Polymers*; Nalwa H. S., Miyama S., Eds.; CRC Press: Boca Raton, FL, 1997.

(3) *Nonlinear Optical Properties of Organic Molecules and Crystals*; Chemla D. S., Zyss J., Eds.; Academic Press: New York, 1987.

(4) (a) LeCours, S. M.; Guan, H. W.; DiMagno, S. G.; Wang, C. H.; Therien, M. J. *J. Am. Chem. Soc.* **1996**, *118*, 1497. (b) Priyadarshy, S.; Therien, M. J.; Beratan, D. *J. Am. Chem. Soc.* **1996**, *118*, 1504.

(5) (a) Blanchard-Desce, M.; Alain, V.; Bedworth, P. V.; Marder, S. R.; Fort, A.; Runser, C.; Barzoukas, M.; Lebus, S.; Wortmann, R. *Chem.—Eur. J.* **1997**, *3*, 1091. (b) Marder, S. R.; Torruellas, W. E.; Blanchard-Desce, M.; Ricci, V.; Stegeman, G. I.; Gilmour, S.; Brédas, J. L.; Li, J.; Bublitz, G. U.; Boxer, S. G. *Science* **1997**, *276*, 1233.

(6) (a) Zyss, J.; Ledoux, I. *Chem. Rev.* **1994**, *94*, 77. (b) Kannan, R.; He, G. S.; Lin, T.-C.; Prasad, P. N.; Vaia, R. A.; Tan, L.-S. *Chem. Mater.* **2004**, *16*, 185. (c) Brunel, J.; Mongin, O.; Jutand, A.; Ledoux, I.; Zyss, J.; Blanchard-Desce, M. *Chem. Mater.* **2003**, *15*, 4139 and references herein. (d) Le Bozec, H.; Le Bouder, T.; Maury, O.; Ledoux, I.; Zyss, J. *J. Opt. A: Pure Appl. Opt.* **2002**, *4*, S 189.

(7) For a recent report exemplifying the 2-D approach, see: Thallapally, P. K.; Desiraju, G. R.; Bagieu-Beucher, M.; Masse, R.; Bourgogne, C.; Nicoud, J.-F. *Chem. Commun.* **2002**, 1052.

10.1021/cm0492989 CCC: $27.50
Published on Web 08/05/2004

Scheme 1

chromophores and "inflating" them by *carbo*merization,[8] or by finding an optimal combination of donor/acceptor strengths for a given bridge that maximizes the NLO response, in relation with the degree of bond length alternation (BLA).[9] More recent years have witnessed a growing interest for molecular-scale devices, in relation to the concept of molecular switches.[10,11] In this context, the incorporation of switchability in NLO materials should lead to various new applications. However, this has been attempted in only a few instances,[12] in particular by changing the oxidation state of a donor (or acceptor) substituent.[13] All together, these examples illustrate the fact that the search for new organic chromophores is a very active research area, which encompasses molecules with greater complexity than those of the substituted stilbene previously investigated.

For instance, azulene is a non-benzenoid aromatic molecule with a polar resonance structure (Scheme 1), which leads to an experimental dipole moment of about 0.8 D.[14] Owing to this electronic feature, azulene appears to be a versatile fragment with either an electron-rich five-membered ring acting as a potential donor or an electron-deficient seven-membered ring acting as a potential electron acceptor. While the electron acceptor character is supported by the reaction with nucleophiles at the seven-membered ring,[15] the electron donor character has been proven by the reaction with electrophiles at the five-membered ring,[15] or by the stabilization of methylcations.[16] Apart from these chemical capabilities, azulene has been attracting a growing interest in various areas of molecular materials, such as conducting polymers,[17−20] charge-transfer complexes,[21,22] molecular switches,[23] and finally NLO materials.[24−29]

The first report on NLO properties for azulene derivatives was the computational investigation of Morley,[30] who suggested in 1988 that azulene is a potential donor fragment, while the first experimental data were reported in 1996, by Asato.[28c] Later on, we reported that 1-(4-nitrophenylazo)azulene possesses a β value of 80×10^{-30} cm^{-5} esu^{-1} (at 1.907 μm), larger than that of Disperse Red One (DR1), the related and well-known stilbene-based chromophore.[27a] These data support the idea that the azulen-1-yl substituent is indeed extremely efficient as an electron donor.

In the present paper, we report on a class of new cationic dyes built up from various 1-methylpyridinium-based substituents as very efficient electron acceptors to fully investigate the electron-donating capabilities of the azulene fragment, and its potential application in nonlinear optics. First, the crystallographic data are used to point out the surprisingly large donating strength exhibited by this pure hydrocarbon fragment by means of correlations between donating strengths and structural data. Then, the quadratic hyperpolarizabilities are investigated by the hyper Rayleigh scattering (HRS) technique,[31,32] and are discussed within the framework of Marder's relationships between molecular geometries and optimized quadratic and cubic NLO response.[9a] The molecular structures of the chromophores under investigation in the present study are presented in Scheme 2.

Experimental Section

Starting Materials and Equipment. The starting materials and solvent were used without further purification. Azulenecarboxaldehyde was synthesiszed as previously described.[31] Elemental analyses were performed by the Service de Microanalyses du Laboratoire de Chimie de Coordination, in Toulouse. The NMR spectra were registered on a Bruker AM 250 or on a Bruker AMX400 when complete assignment of the ^{1}H and ^{13}C NMR spectra of all the compounds required 1D and 2D ^{1}H−^{1}H COSY, HMQC ^{1}H−^{13}C, and HMBC ^{1}H−^{13}C experiments. The atom labeling used for the assignment is given in Scheme 2. Electronic spectra were recorded on a Hewlett-Packard 8452 A spectrophotometer.

Synthesis. *Azulene-1-azo(N-methyl-4′-pyridinium) Iodide (**1**$^+I^-$)* was synthesized as previously described.[34] The compound was then turned to the hexafluorophosphate salt by metathesis. Single crystals were obtained by slow diffusion of diethyl ether in a solution of the hexafluorophosphate derivative in acetonitrile.

(8) (a) Ducere, J. M.; Lepetit, C.; Lacroix, P. G.; Heully, J. L.; Chauvin, R. *Chem. Mater.* **2002**, *14*, 3332. (b) Lepetit, C.; Lacroix, P. G.; Peyrou, V.; Saccavini, C.; Chauvin, R. *J. Comput. Methods Sci. Eng.*, in press.
(9) (a) Meyers, F.; Marder, S. R.; Pierce, B. M.; Brédas, J. L. *J. Am. Chem. Soc.* **1994**, *116*, 10703. (b) Marder, S. R.; Gorman, C. B.; Tiemann, B. G.; Cheng, L. T. *J. Am. Chem. Soc.* **1993**, *115*, 3006.
(10) Lehn, J. M. *Supramolecular Chemistry—Concepts and Perspectives*; VCH: Weinheim, Germany, 1995.
(11) (a) Ward, M. D. *Chem. Soc. Rev.* **1995**, *24*, 121. (b) Delaire, J. A.; Nakatani, K. *Chem. Rev.* **2000**, *100*, 1817.
(12) Coe, B. J. *Chem.—Eur. J.* **1999**, *5*, 2464.
(13) Coe, B. J.; Houbrechts, S.; Asselberghs, I.; Persoons, A. *Angew. Chem., Int. Ed.* **1999**, *38*, 366.
(14) Tobler, H. J.; Bauder, A.; Gunthard, H. H. *J. Mol. Spectrosc.* **1965**, *18*, 239.
(15) Zeller, K. P. In *Houben Weyl, Methoden der Organischen Chemie*; Thieme: Stuttgart, Germany, 1985; Vol. 5/2c, p 127.
(16) Ito, S.; Kikuchi, S.; Morita, N.; Asao, T. *Chem. Lett.* **1996**, 175.
(17) Redl, F. X.; Köthe, O.; Röckl, K.; Bauer, W.; Daub, J. *Macromol. Chem. Phys.* **2000**, *201*, 2091.
(18) Porsch, M.; Sigl-Seifert, G.; Daub, J. *Adv. Mater.* **1997**, *9*, 635.
(19) Bargon, J.; Mohmand, S.; Waltman, R. J. *Mol. Cryst. Liq. Cryst.* **1983**, *93*, 279.
(20) Tourillon, G.; Garnier, F. *J. Electroanal. Chem.* **1982**, *135*, 173.
(21) Schmitt, S.; Baumgarten, M.; Simon, J.; Hafner, K. *Angew. Chem., Int. Ed.* **1998**, *37*, 1077.
(22) Frey, J. E.; Andrews, A. M.; Combs, S. D.; Edens, S.P.; Puckett, J. J.; Seagle, R. E.; Torreano, L. A. *J. Org. Chem.* **1992**, *57*, 6460.
(23) Mrozek, T.; Görner, H.; Daub, J. *Chem.—Eur. J.* **2001**, *7*, 1028.
(24) Zhou, X.; Ren, A. M.; Feng, J. K.; Xiao, X. J.; Shu, C. C. *Chin. J. Chem.* **2004**, *22*, 38.
(25) Lambert, C.; Nöll, G.; Zabel, M.; Hampel, F.; Schmälzlin, E.; Bräuchle, C.; Meeholz, K. *Chem.—Eur. J.* **2003**, *9*, 4232.
(26) Farrel, T.; Meyer-Friedrichsen, T.; Malessa, M.; Haase, D.; Saak, W.; Asselberghs, I.; Wostyn, K.; Clays, K.; Persoons, A.; Heck, J.; Manning, A. R. *J. Chem. Soc., Dalton Trans.* **2001**, 29.
(27) (a) Lacroix, P. G.; Malfant, I.; Iftime, G.; Razus, A. C.; Nakatani, K.; Delaire, J. A. *Chem.—Eur. J.* **2000**, *6*, 2599. (b) Iftime, G.; Lacroix, P. G.; Nakatani, K.; Razus, A. C. *Tetrahedron Lett.* **1998**, *39*, 6853.
(28) (a) Woodford, J. N.; Wang, C. H.; Asato, A. E.; Liu, R. S. H. *J. Chem. Phys.* **1999**, *111*, 4621. (b) Wang, P.; Zhu, P.; Ye, C.; Asato, A. E.; Liu, R. S. H. *J. Phys. Chem. A* **1999**, *103*, 7076. (c) Asato, A. E.; Liu, R. S. H.; Rao, V. P.; Cai, Y. M. *Tetrahedron Lett.* **1996**, *37*, 419.
(29) Herrmann, R.; Pedersen, B.; Wagner, G.; Youn, J. H. *J. Organomet. Chem.* **1998**, *571*, 261.
(30) (a) Morley, J. O. *J. Am. Chem. Soc.* **1988**, *110*, 7660. (b) Morley, J. O. *J. Chem. Soc., Perkin Trans. 2* **1989**, 103.
(31) (a) Clays, K.; Persoons, A. *Rev. Sci. Instrum.* **1992**, *63*, 3285. (b) Hendrickx, E.; Clays, K.; Persoons, A. *Acc. Chem. Res.* **1998**, *31*, 675.
(32) Terhune, R. W.; Maker, P. D.; Savage, C. M. *Phys. Rev. Lett.* **1965**, *14*, 681.
(33) Hafner, K.; Bernhard, U. C. *Angew. Chem.* **1957**, *69*, 533.
(34) Razus, A. C.; Birzan, L.; Nae, S.; Razus, S. A.; Cimpeanu, V.; Stanciu, C. *Synth. Commun.* **2002**, *32*, 825.

Scheme 2

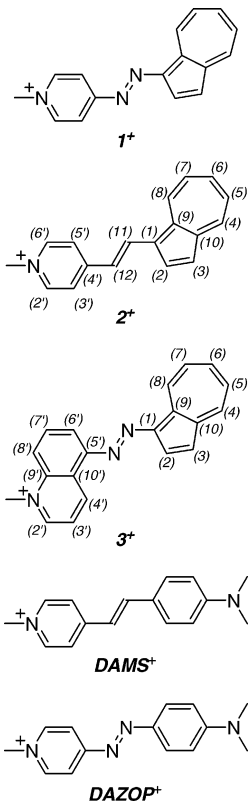

*1-[(E)-2-(N-Methyl-4′-pyridinium)ethenyl]azulene Iodide (**2**$^+I^-$).* *N*-Methylpicolinium iodide was generated as a pale yellow solid from 4-picoline (930 mg, 10^{-2} mol) and iodomethane (1.7 g, 1.2 10^{-2} mol) by fast mixing in a small flask. After a few minutes, the flask was connected to the vacuum line to remove the excess of iodomethane. One part of this salt (235 mg, 10^{-3} mol) was dissolved in 30 mL of 2-propanol, with 156 mg (10^{-3} mol) of azulenecarboxaldehyde, and 1 drop of piperidine. The resulting solution was refluxed overnight. After cooling, the large amount of formed solid was filtered off, washed with 2-propanol, and dried under vacuum (347 mg, yield 93%). Anal. Calcd (Found) for $C_{18}H_{16}IN$: C, 57.92 (57.45); H, 4.32 (4.00); N, 3.75 (3.68). ^{1}H NMR (DMSO-d_6): δ 4.20 (s, 3H, *N*-CH_3), 7.44 (d, J = 15.9 Hz, 1H, H(12)), 7.45 (t, J = 9.5 Hz, 1H, H(5)), 7.49 (t, J = 9.8 Hz, 1H, H(7)), 7.58 (d, J = 4.3 Hz, 1H, H(3)), 7.87 (t, J = 9.8 Hz, 1H, H(6)), 8.23 (d, J = 6.8 Hz, 2H, H(3′,5′)), 8.47 (d, J = 4.3 Hz, 1H, H(2)), 8.50 (d, J = 9.3 Hz, 1H, H(4)), 8.69 (d, J = 15.8 Hz, 1H, H(11)), 8.73 (d, J = 6.8 Hz, 2H, H(2′,6′)), 9.10 (d, J = 9.8 Hz, 1H, H(8)). ^{13}C NMR (DMSO-d_6): δ 47.25 (*N*-CH_3), 120.28 (C(12)), 121.85 (C(3)), 123.04 (C(3′,5′)), 126.61 (C(1)), 126.84 (C(7)), 127.81 (C(5)), 134.08 (C(11)), 135.32 (C(2)), 136.15 (C(8)), 139.25 (C(4)), 139.77 (C(9)), 140.97 (C(6)), 145.10 (C(2′,6′)), 145.30 (C(10)), 154.30 (C(4′)). The compound was then turned to the trifluoromethanesulfonate salt by metathesis. Single crystals were obtained by slow diffusion of diethyl ether in a solution of the triflate derivative in acetonitrile.

*Azulene-1-azo[(N-methyl-5′-quinolinium)] Iodide (**3**$^+I^-$).* Phosphoric acid (85%, 0.9 mL) and nitric acid (65%, 0.6 mL) were added to 5-aminoquinoline (216 mg, 1.5 × 10^{-3} mol) at −6 °C. The mixture was stirred for 15 min at room temperature until complete dissolution. Then, the solution was cooled to −6 °C, and solid sodium nitrite (104 mg, 1.5 × 10^{-3} mol) was slowly added in 5 min. After addition of 15 g of crushed ice, the solution was added at 0 °C to a suspension of azulene (193 mg, 1.5 × 10^{-3} mol) and potassium acetate (6 g) in 75 mL of ethanol. The resulting red mixture was stirred for 15 min at 0 °C, followed by the addition of 15 mL of aqueous sodium carbonate (20%). The solution was extracted with dichloromethane (3 × 75 mL). The combined organic layers were washed with water and dried (Na_2SO_4), and the solvent was evaporated off. The compound was purified by chromatography on alumina (the eluent was *n*-pentane for the unreacted azulene and then dichloromethane for the product), which yielded 380 mg (89%) of azulene-1-azo(5′-quinoline). ^{1}H NMR (DMSO-d_6): δ 7.59 (t, J = 9.7 Hz, 1H), 7.64 (d, J = 4.8 Hz, 1H), 7.68−7.73 (m, 2H), 7.91 (dd, J = 8.2 and 7.8 Hz, 1H), 8.01 (t, J = 9.8 Hz, 1H), 8.13 (m, 2H), 8.47 (d, J = 4.6 Hz, 1H), 8.62 (d, J = 9.3 Hz, 1H), 9.02 (dd, J = 4.1 and 1.6 Hz, 1H), 9.36 (br d, J = 8.7 Hz, 1H), 9.41 (d, J = 9.8 Hz, 1H).

To 283 mg (10^{-3} mol) of this compound in solution in 175 mL of chloroform was added 9.5 mL of methyl iodide. The reaction mixture was refluxed for 30 min, and then a new amount of methyl iodide was added (5 mL). After an additional 2 h of reflux, a second supplementary quantity of methyl iodide was added (5 mL), and reflux was maintained overnight. The resulting mixture was evaporated to dryness under reduced pressure, leading to a lilac-black microcrystalline compound (410 mg, 96%). Anal. Calcd (Found) for $C_{20}H_{16}F_6N_3P$: C, 54.18 (54.36); H, 3.64 (3.44); N, 9.48 (8.96). ^{1}H NMR (DMSO-d_6): δ 4.71 (s, 3H, *N*-CH_3), 7.71 (d, J = 4.5 Hz, 1H, H(3)), 7.72 (t, J = 9.8 Hz, 1H, H(5)), 7.82 (t, J = 9.7 Hz, 1H, H(7)), 8.11 (t, J = 10.0 Hz, 1H, H(6)), 8.26 (dd, J = 8.5 and 5.7 Hz, 1H, H(3′)), 8.38 (bt, J = 8.2 Hz, 1H, H(7′)), 8.47 (d, J = 7.6 Hz, 1H, H(8′)), 8.51 (d, J = 8.9 Hz, 1H, H(6′)), 8.55 (d, J = 4.4 Hz, 1H, H(2)), 8.70 (d, J = 9.2 Hz, 1H, H(4)), 9.46 (d, J = 9.9 Hz, 1H, H(8)), 9.64 (d, J = 5.4 Hz, 1H, H(2′)), 10.19(d, J = 8.5 Hz, 1H, H(4′)). ^{13}C NMR (DMSO-d_6): δ 46.64 (*N*-CH_3), 114.63 (C(8′)), 119.58 (C(6′)), 122.78 (C(3′)), 123.05 (C(3)), 126.06 (C(2)), 127.90 (C(10′)), 130.65 (C(7)), 130.77 (C(5)), 136.34 (C(7′)), 136.71 (C(8)), 139.87 (C(9′)), 141.19 (C(4)), 141.65 (C(9)), 142.51 (C(6)), 143.99 (C(4′)), 145.52 (C(1)), 146.33 (C(10)), 149.71 (C(5′)), 151.38 (C(2′)). The compound was then turned to the hexafluorophosphate salt by metathesis. Single crystals were obtained by slow diffusion of diethyl ether in a solution of the hexafluorophosphate derivative in acetonitrile.

4-(Dimethylamino)azo(N-methyl-4′-pyridinium) iodide (DAZOP$^+I^-$) was synthesized as previously described[35] and then turned into the hexafluorophosphate derivative by metathesis. Anal. Calcd (Found) for $C_{14}H_{17}F_6N_4P$: C, 43.41 (43.74); H, 4.42 (4.01); N, 14.46 (14.22). Single crystals were obtained by slow diffusion of diethyl ether in a solution of the hexafluorophosphate derivative in acetonitrile.

Metathesis. (i) For PF_6^-. The iodide salts were dissolved in the minimum of water, and a large amount of a saturated aqueous solution of ammonium hexafluorophosphate was added until no more precipitation occurred. The precipitates were filtered off, rinsed with water, and dried in a desiccator.

(ii) For NO_3^-. The iodide salts were dissolved in the minimum of water, and a stoichiometric amount of an aqueous solution of $AgNO_3$ was added. A white suspension of AgI was filtered off. The solutions were evaporated to dryness and then crystallized in ethanol.

(iii) For BF_4^-, BPh_4^-, and $CF_3SO_3^-$. The iodide salts were dissolved in the minimum of water, and a large amount of a saturated aqueous solution of $NaBF_4$, $NaBPh_4$, or KCF_3SO_3 was added. The resulting precipitates were filtered off, rinsed with water, dried, and crystallized in ethanol.

Structure Analysis and Refinement. The data were collected on a Stoe imaging plate diffraction system (IPDS), equipped with an Oxford Cryosystems cryostream cooler device and using graphite-monochromated Mo Kα radiation (λ = 0.71073 Å), for **1**$^+PF_6^-$ and **3**$^+PF_6^-$. Data sets for **2**$^+CF_3SO_3^-$ and DAZOP$^+PF_6^-$ were collected on a Kuma Oxford Diffraction four-circle κ geometry goniometer, equipped with a CCD detector and coupled with an Oxford Instruments cryojet low-*T* device. The data were collected at 160 K, except for DAZOP$^+$-PF_6^- (room temperature). For each structure, final unit cell parameters were obtained by means of a least-squares refinement of a set of well-measured reflections. No significant fluctuations of intensities were observed during the measurements. The structures were solved by means of direct methods

(35) Coradin, T.; Clément, R.; Lacroix, P. G.; Nakatani, K. *Chem. Mater.* **1996**, *8*, 2153.

Table 1. Crystal Data for $1^+PF_6^-$, $2^+CF_3SO_3^-$, $3^+PF_6^-$, and $DAZOP^+PF_6^-$

	$1^+PF_6^-$	$2^+CF_3SO_3^-$	$3^+PF_6^-$,	$DAZOP^+PF_6^-$
		Crystal Data		
empirical formula	$C_{16}H_{14}F_6N_3P$	$C_{19}H_{16}F_3NO_3S$	$C_{20}H_{16}F_6N_3P$	$C_{14}H_{17}F_6N_4P$
fw	393.27	395.39	443.33	386.29
cryst size (mm)	0.32 × 0.18 × 0.08	0.17 × 0.12 × 0.09	0.25 × 0.12 × 0.10	0.30 × 0.17 × 0.06
cryst syst	monoclinic	monoclinic	triclinic	monoclinic
space group	$P2_1/c$	$P2_1/c$	$P\bar{1}$	$P2_1/a$
a (Å)	11.355(2)	12.7486(16)	7.8976(11)	11.4181(13)
b (Å)	9.388(2)	11.4058(15)	10.8659(16)	7.5574(8)
c (Å)	15.734(3)	13.7122(18)	12.1852(17)	19.0355(17)
α (deg)	90	90	88.871(17)	90
β (deg)	105.45(3)	116.656(13)	74.119(16)	97.886(8)
γ (deg)	90	90	68.934(16)	90
V (Å^3)	1616.6(5)	1781.9(4)	934.9(2)	1627.1(3)
d_{calcd} (Mg/m^3)	1.616	1.474	1.575	1.577
μ(Mo Kα) (cm^{-1})	0.240	0.232	0.218	0.238
T (K)	160	160	160	293
		Data Collection		
radiation (Mo Kα) (Å)	0.71073	0.71073	0.71073	0.71073
scan mode	ϕ	ω	ϕ	ω
scan range (deg)	0−200.2		0−251.2	
2θ range (deg)	2.9−48.4	6.0−56.4	5.1−52.2	6.5−64.4
no. of reflns				
measured	9958	14284	8926	15571
unique	2515	4411	3398	5368
used	2515	4411	3398	5368
		Refinement		
refinement on	F^2	F^2	F^2	F^2
no. of variables	290	253	326	283
H atom treatment	calcd	calcd	calcd	calcd
R [$I > 2\sigma(I)$]	0.0379	0.0698	0.0359	0.0544
wR	0.0727	0.1358	0.0816	0.1363
$\Delta\rho_{max}$ (e Å^{-3})	0.192	0.653	0.191	0.440
$\Delta\rho_{min}$ (e Å^{-3})	−0.180	−0.323	−0.192	−0.286
GOF	0.912	0.947	0.955	0.922

using the program SIR92[36] and subsequent difference Fourier maps and then refined by least-squares procedures on F^2 by using SHELXL-97,[37] included in the WinGX programs.[38] The crystallographic data are summarized in Table 1. Atomic scattering factors were taken from the *International Tables for X-ray Crystallography*.[39] All hydrogen atoms were located on a difference Fourier map but introduced in the refinement as fixed contributors, using a riding model with an isotropic thermal parameter fixed at 20% higher than those of the C sp^2 atoms and 50% for the C sp^3 atoms, and the methyl groups were refined with the torsion angle as a free variable. All nonhydrogens atoms were anisotropically refined, and in the last cycles of refinement weighting schemes have been used, where weights were calculated from the following formula: $W = 1/[\sigma^2(F_o^2) + (aP)^2 + bP]$, where $P = (F_o^2 + 2F_c^2)/3$. For $1^+PF_6^-$, $3^+PF_6^-$, and $DAZOP^+PF_6^-$, fluorine atoms were found statistically disordered and were refined with a ratio of occupancy equal to 50%/50% for $1^+PF_6^-$ and $3^+PF_6^-$ and 57%/43% for $DAZOP^+PF_6^-$. Criteria for a satisfactory complete analysis were the ratios of the root-mean-square shift standard deviation being less than 0.1 and no significant features in the final difference Fourier maps. Drawings of molecules were performed by using the program ORTEP3[40] with 50% probability displacement ellipsoids for non-hydrogen atoms. Crystallographic data have been deposited with the Cambridge Crystallographic Data Centre as supplementary publication nos. CCDC 237695−237698 for $1^+PF_6^-$, $2^+CF_3SO_3^-$, $3^+PF_6^-$, and $DAZOP^+PF_6^-$, respectively.

Theoretical Methods. The all-valence INDO (intermediate neglect of differential overlap) method[41] was employed for the calculation of the electronic features of the chromophores. Calculations were performed using the INDO/1 Hamiltonian incorporated in the commercially available MSI software package ZINDO.[42]Structural parameters used for the calculations were taken from the present X-ray structures for 1^+, 2^+, and $DAZOP^+$, and from a previously reported structure for $DAMS^+$.[43] The cubic hyperpolarizabilities (γ) were calculated with the PS3 Hamiltonian incorporated in the MSI software package MOPAC.[44]

NLO Measurements. Second harmonic generation (SHG) measurements in the solid state were carried out by the Kurtz−Perry powder test,[45] using a nanosecond-pulsed Nd:YAG (10 Hz) laser. The fundamental radiation was used as the incident laser beam for SHG. The second harmonic signal was detected by a photomultiplier, and read on an ultrafast Tektronic TDS 620B oscilloscope. The samples were uncalibrated microcrystalline powders obtained by grinding and put between two glass plates.

Details of the HRS experiment have been discussed elsewhere.[31,46] The measurements have been performed by femtosecond HRS at 800 nm, in acetonitrile. The reference was Crystal Violet chloride in methanol, for which β_{xxx} is equal to 338×10^{-30} cm^5 esu^{-1}.[47] The difference in symmetry (octupolar for the reference and dipolar for the azulene derivatives) and

(36) SIR92−A program for crystal structure solution: Altomare, A.; Cascarano, G.; Giacovazzo, C.; Guagliardi, A. *J. Appl. Crystallogr.* **1993**, *26*, 343.
(37) SHELX97−Programs for Crystal Structure Analysis (Release 97-2): G. M. Sheldrick, Institüt für Anorganische Chemie der Universität, Tammanstrasse 4, D-3400 Göttingen, Germany, 1998.
(38) WINGX − Farrugia, L. J. *J. Appl. Crystallogr.* **1999**, *32*, 837.
(39) *International Tables for X-ray Crystallography*; Kynoch Press: Birmingham, England, 1974; Vol. IV.
(40) ORTEP3 for Windows: Farrugia, L. J. *J. Appl. Crystallogr.* **1997**, *30*, 565.
(41) (a) Zerner, M. C.; Loew, G.; Kirchner, R.; Mueller-Westerhoff, U. *J. Am. Chem. Soc.* **1980**, *102*, 589. (b) Anderson, W. P.; Edwards, D.; Zerner, M. C. *Inorg. Chem.* **1986**, *25*, 2728.
(42) *ZINDO*, release 96.0; Molecular Simulations Inc.: Cambridge, U.K., 1996.
(43) Lu, T. H.; Lee, T. J.; Wong, C.; Kuo, K. T. *J. Chin. Chem.* **1979**, *26*, 53.
(44) *MOPAC*, release 96.0; Molecular Simulations Inc.: Cambridge, U.K., 1996.
(45) (a) Kurtz, S. K.; Perry, T. T. *J. Appl. Phys.* **1968**, *39*, 3798. (b) Dougherty, J. P.; Kurtz, S. K. *J. Appl. Crystallogr.* **1976**, *9*, 145.
(46) Hendrickx, E.; Clays, K.; Persoons, A.; Dehu, C.; Brédas, J. L. *J. Am. Chem. Soc.* **1995**, *117*, 3547.

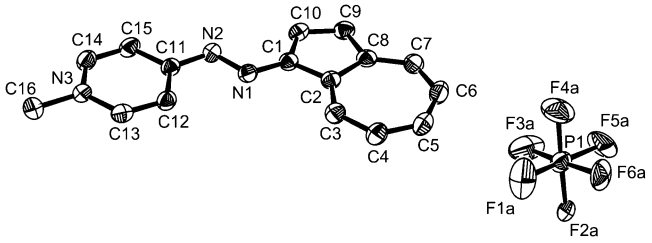

Figure 1. Atom labeling scheme for $\mathbf{1}^{+}PF_6^{-}$. Hydrogen atoms are omitted for clarity.

the difference in local optical fields (methanol versus acetonitrile) have been taken into account. None of the samples show multiphonon fluorescence at 400 nm, when excited at 800 nm (vide infra). This observation is in accordance with the previous report by Woodford et al.[28a]

Results and Discussion

Design and General Features. The synthesis of 1-(4-R-phenylazo)azulenes is readily obtained in one step, by reaction of azulene with the appropriate diazonium salt, following a procedure reported many years ago.[48] This route is suitable for linking azulene to various substituted phenyl groups. The procedure is used here in the case of pyridine and quinoline, which are modest acceptor fragments, but can be turned into strong ones ($\mathbf{1}^{+}$, $\mathbf{3}^{+}$) by methylation. By contrast, the synthesis of 1-[2-(phenyl)ethenyl]azulene is difficult, and requires a two-step synthesis in a dry atmosphere, the resulting compound being a mixture of *E*/*Z* isomers.[27b] Nevertheless, the related methylpyridinium derivative $\mathbf{2}^{+}$ is readily obtained, following a procedure first reported by Kung.[49] Both routes lead to compounds in which the azulene fragment is linked to an aromatic acceptor unit through a conjugated carbon (or nitrogen) based bridge. The question of whether the azo linkage is better than the ethenyl one for NLO purposes is somewhat controversial. Nicoud et al. have reported that replacing a carbon by a nitrogen usually decreases the NLO response.[50] By contrast, Morley has predicted that azobenzenes should exhibit larger hyperpolarizabilities than stilbene analogues in some cases,[51] even if this has usually not been reported experimentally.[52] In any case, it is interesting to point out here that both classes of chromophores may be readily accessible in the azulenepyridinium series.

Description of the Structures. Figures 1−4 illustrate the atomic numbering scheme employed for molecules $\mathbf{1}^{+}PF_6^{-}$, $\mathbf{2}^{+}CF_3SO_3^{-}$, $\mathbf{3}^{+}PF_6^{-}$, and DAZOP^{+}-PF_6^{-}, respectively. The crystal structure of $\mathbf{1}^{+}PF_6^{-}$ reveals a single molecule in the asymmetric unit cell. The $\mathbf{1}^{+}$ cation is nearly planar, with the largest deviation of 0.119 Å observed at C(7). The angle between the molecular plane and the 2_1 crystallographic axis is equal to 43°, which leads to a crystal packing arising from two nearly orthogonal layers of $\mathbf{1}^{+}$ cations. A single molecule is present in the asymmetric unit cell of $\mathbf{2}^{+}CF_3SO_3^{-}$. The cation is planar, with the largest deviation of 0.116 Å observed at C(17). The compound crystallizes in the same $P2_1/c$ space group as $\mathbf{1}^{+}PF_6^{-}$. Due to the same cation shape, one might have expected both derivatives to be isostructural. In fact, the planes of the $\mathbf{2}^{+}$ cations are nearly parallel to the 2_1 axis, in the present case, which leads to a structure in which all the cations are roughly parallel. The crystal cell of $\mathbf{3}^{+}PF_6^{-}$ is built up from two molecules, which refer to each other by an inversion center. The $\mathbf{3}^{+}$ cation is almost perfectly planar, with the largest deviation of 0.105 Å observed at C(10). Due to the $\bar{1}$ symmetry, all the cations are strictly parallel in the crystal. Finally, DAZOP$^{+}PF_6^{-}$ reveals a single molecule in its asymmetric unit cell. The cation is planar, with the largest deviation of 0.150

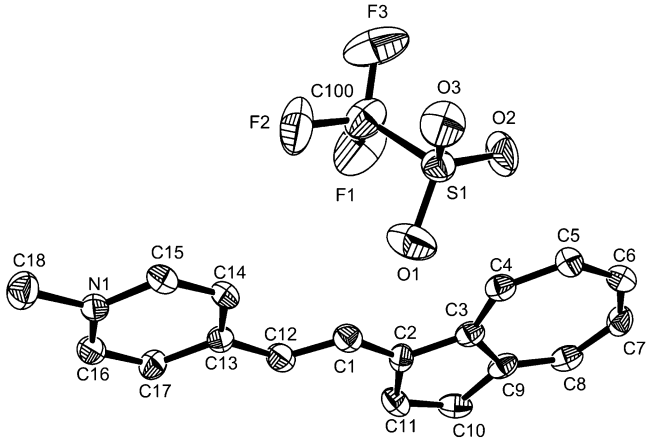

Figure 2. Atom labeling scheme for $\mathbf{2}^{+}CF_3SO_3^{-}$. Hydrogen atoms are omitted for clarity.

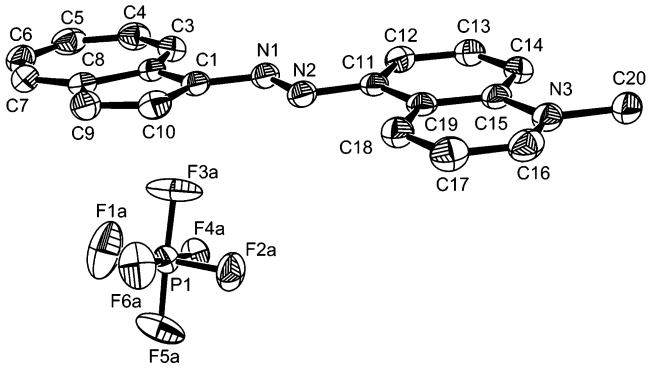

Figure 3. Atom labeling scheme for $\mathbf{3}^{+}PF_6^{-}$. Hydrogen atoms are omitted for clarity.

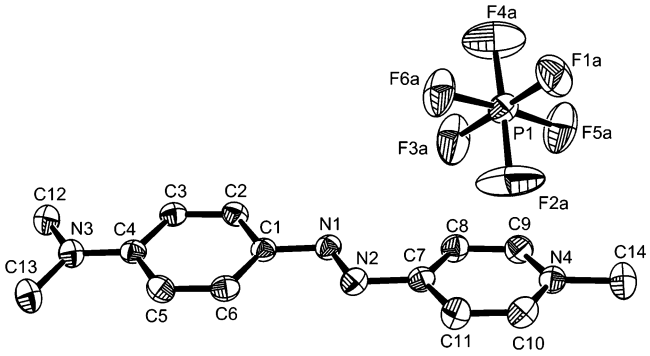

Figure 4. Atom labeling scheme for DAZOP$^{+}PF_6^{-}$. Hydrogen atoms are omitted for clarity.

(47) Olbrechts, G.; Strobbe, R.; Clays, K.; Persoons, A. *Rev. Sci. Instrum.* **1998**, *69*, 2233.
(48) (a) Anderson, A. G.; Nelson, J. A.; Tazuma, J. J. *J. Am. Chem. Soc.* **1953**, *75*, 4980. (b) Gerson, F.; Heilbronner, E. *Helv. Chim. Acta* **1958**, *41*, 1444. (c) Gerson, F.; Schultze, J.; Heilbronner, E. *Helv. Chim. Acta* **1958**, *41*, 1463.
(49) Kung, T. K. *J. Chin. Chem. Soc.* **1978**, *25*, 131.
(50) Nicoud, J. F.; Twieg, R. J. In ref 3, p 277.
(51) Morley, J. O. *J. Chem. Soc., Perkin Trans. 2* **1995**, 731.
(52) Cheng, L. T.; Tam, W.; Stevenson, S. H.; Meredith, G. R.; Rikken, G.; Marder, S. R. *J. Phys. Chem.* **1991**, *95*, 10631.

Scheme 3

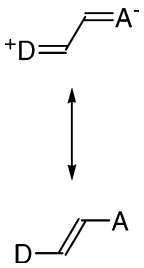

Å observed at C(13). The angle between the molecular plane and the 2_1 axis is equal to 38°, which leads to two sublayers of nearly perpendicular DAZOP$^+$ units.

In a simple two-level description, the ground state of donor−acceptor conjugated molecules can be rationalized in terms of a linear combination of two resonance forms (Scheme 3).[53] For sets of extremely modest donor−acceptor substituents, no charge transfer takes place in the molecules, and therefore, the ground-state geometry is mostly that of the neutral form only (bottom of Scheme 3). As the donor−acceptor strength increases, the charge-separated resonance form (top of Scheme 3) contributes more to the ground-state geometry. The major consequence of this effect is to gradually increase the length of the central double bond of the chromophores. Therefore, the measure of this bond may tentatively be used to evaluate the donor−acceptor capabilities of substituents. These values are equal to 1.295(9) Å (−N═N−), 1.344(5) Å (−CH═CH−), 1.274-(6) Å (−N═N−), and 1.277(5) Å (−N═N−) for **1**$^+$, **2**$^+$, **3**$^+$, and DAZOP$^+$, respectively.

In the case of azo(*N*-methyl-4′pyridinium) derivatives, very few data are available,[54] and therefore, no correlation can be established. Nevertheless, it is interesting to point out that the longest N═N double bond reported in the serie is that of **1**$^+$, in support of a large electron donor strength for the azulene fragment. By contrast, many more crystal structures have been solved in the stilbazolium series, which therefore offers a better route for a relevant comparison.[55] Representative data are gathered in Figure 5. A relationship can be established between the C═C bond length of the ethenyl bridge and the σ_p^+ Hammet constant[56] of the 4′-substituted group. On the basis of this correlation, the azulene in **2**$^+$ appears to exhibit a higher electron donor efficiency than that of a (dimethylamino)phenyl group. Therefore, and according to the traditional approach for "push−pull" chromophores, one must expect a larger NLO response for the azulene derivatives than for their stilbazolium analogues. This will be discussed in the next section.

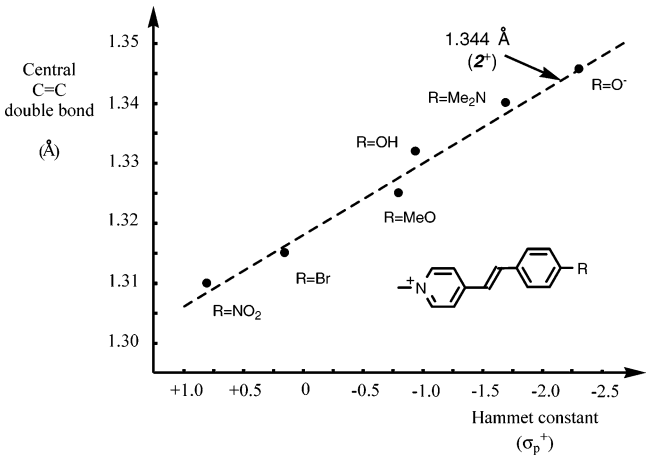

Figure 5. Structural correlation between the donor strengths (σ_p^+) and the ethenyl C═C bond lengths in stilbazolium derivatives. Crystal data are from ref 53.

Table 2. Solid-State Powder Efficiencies (Referred to Urea) for the 1$^+$, 2$^+$, and 3$^+$ Chromophores Combined with Various Anions

chromophore	anion	efficiency	chromophore	anion	efficiency
1$^+$	I^-	0	***3***$^+$	I^-	0
	PF_6^-	0		PF_6^-	0
	NO_3^-	0.3		NO_3^-	0.15
	BF_4^-	0		BF_4^-	0
	BPh_4^-	0		BPh_4^-	3.5
	$CF_3SO_3^-$	0		$CF_3SO_3^-$	0
2$^+$	I^-	0			
	PF_6^-	0			
	NO_3^-	0			
	BF_4^-	0			
	BPh_4^-	0.15			
	$CF_3SO_3^-$	0			

NLO Properties. At the bulk level, the powder efficiencies in SHG have been tested by the Kurtz−Perry technique[45] for the 18 azulene-based salts available. The data are gathered in Table 2. Surprisingly, a large majority of them (14 compounds) are SHG silent, which reveals a clear tendency for centrosymmetric crystallization. This observation strongly contrasts with our previous investigation of (phenylazo)azulene.[27] Three samples actually exhibit SHG signals in the range 0.15−0.3 times that of urea. However, it has previously been observed that stilbazolium derivatives can exhibit SHG efficiencies up to 1000 times that of urea.[57] Therefore, it cannot be excluded that the present SHG signals to some extent arise from impurities rather than from an intrinsic noncentrosymmetry. Finally, the only sample exhibiting a sizable signal is **3**$^+BPh_4^-$, with an efficiency 3.5 times that of urea. Nevertheless, our attempts to get suitable crystal structures for this compound were unsuccessful.

At the molecular level, the experimental quadratic hyperpolarizabilities of the azulene derivatives are gathered in Table 3, and compared to those of stilbazolium-based analogues. It is important to notice that the values are not overestimated due to multiphoton fluorescence. This is experimentally verified by performing femtosecond hyper Rayleigh scattering experiments as a function of modulation frequency.[47] The finite

(53) Barzoukas, M.; Fort, A.; Blanchard-Desce, M. *New J. Chem.* **1997**, *21*, 309.

(54) Evans, J. S. O.; Benard, S.; Yu. P.; Clément, R. *Chem. Mater.* **2001**, *13*, 3813.

(55) (a) Malfant, I.; Cordente, N.; Lacroix, P. G.; Lepetit, C. *Chem. Mater.* **1998**, *10*, 4079. (b) Marder, S. R.; Perry, J. W.; Yakymyshyn, C. P. *Chem. Mater.* **1994**, *6*, 1137. (c) Li, S. J.; Zhang, D. C.; Huang, Z. L.; Zhang, Y. Q.; Yu, K. B. *Acta Crystallogr., Sect. C: Cryst. Struct. Commun.* **2000**, *56*, 1122. (d) Ziolo, R. F.; Gunther, W. H. H.; Meredith, G. R.; Williams, D. J.; Troup, J. M. *Acta Crystallogr., Sect. B: Struct. Cryst. Cryst. Chem.* **1982**, *38*, 341. (e) Bryant Jn., G. L.; Yakymyshyn, C. P.; Stewaet, K. R. *Acta Crystallogr., Sect. C: Cryst. Struct. Commun.* **1993**, *49*, 350. (f) De Ridder, D. J. A.; Heijdenrijk, D.; Schenk, H.; Dommisse, R. A.; Lemiere, G. L.; Lepoivre, J. A.; Alderweireldt, F. A. *Acta Crystallogr., Sect. C: Cryst. Struct. Commun.* **1990**, *46*, 2197.

(56) Hansch, C.; Leo, A.; Taft, R. W. *Chem. Rev.* **1991**, *91*, 165.

(57) Marder, S. R.; Perry, J. W.; Schaefer, W. P. *Science* **1989**, *245*, 626.

Table 3. Experimental Hyperpolarizabilities (10^{-30} cm^5 esu^{-1}) for Azulene-Based Chromophores, versus Stilbazolium Analogues, Recorded using the Hyper Rayleigh Scattering Method at 800 nm (β) and at Zero Frequency (β_0)[a]

azulene				stilbazolium			
	λ_{max}	b	β_0		λ_{max}	b	β_0
1$^+$	503	192	67	DAZOP$^+$	549	329	154
2$^+$	477	400	108	DAMS$^+$ [b]	470	442	110
3$^+$	501	234	80				

[a] The absorption maxima (λ_{max}) are given in nanometers. [b] Data for DAMS$^+$: Coe, B. J.; Harris, J. A.; Asselberghs, I.; Clays, K.; Olbrechts, G.; Persoons, A.; Hupp, J. T.; Johnson, R. C.; Coles, S. J.; Hursthouse, M. B.; Nakatani, K. *Adv. Funct. Mater.* **2002**, *12*, 110.

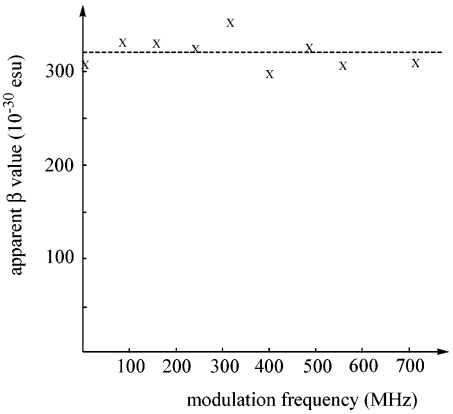

Figure 6. Experimental β values as a function of modulation freqency for DAZOP$^+$PF$_6^-$ indicating the frequency-independent response of the multiphoton-fluorescence-free HRS signal.

lifetime that is associated with any fluorescence results in a demodulation (reduction of amplitude) for higher frequencies.[58] As is exemplified in Figure 6, in the case of DAZOP$^+$PF$_6^-$, no such demodulation is observed, indicating that the HRS signal is not comprised of any multiphoton fluorescence contribution.[59] A similar frequency-independent signal (within experimental error 0×10^{-30} esu/MHz slope for β as a function of modulation frequency) was observed for the other compounds also. In Table 3, the experimental β values are enhanced by resonance, as the second harmonic (400 nm) is close to the absorption maximum (λ_{max}). Therefore, the parameter to take into account for a relevant comparison is the static hyperpolarizability (β_0), extracted from the widely used two-level description of the NLO response of push−pull organic chromophores, according to the following equation:[60]

$$\beta = \frac{3e^2\hbar^2 f_{ge}(\Delta\mu)_{ge}}{2mE_{ge}^3} \times \frac{E_{ge}^4}{(E_{ge}^2 - (2\hbar\omega)^2)(E_{ge}^2 - (\hbar\omega)^2)} \quad (1)$$

in which the first part on the right-hand side is β_0, independent of the energy $\hbar\omega$ of the incident laser beam. Within this model, a single transition between the ground state (g) and a low-lying excited state (e) is responsible for most of the NLO response, β being

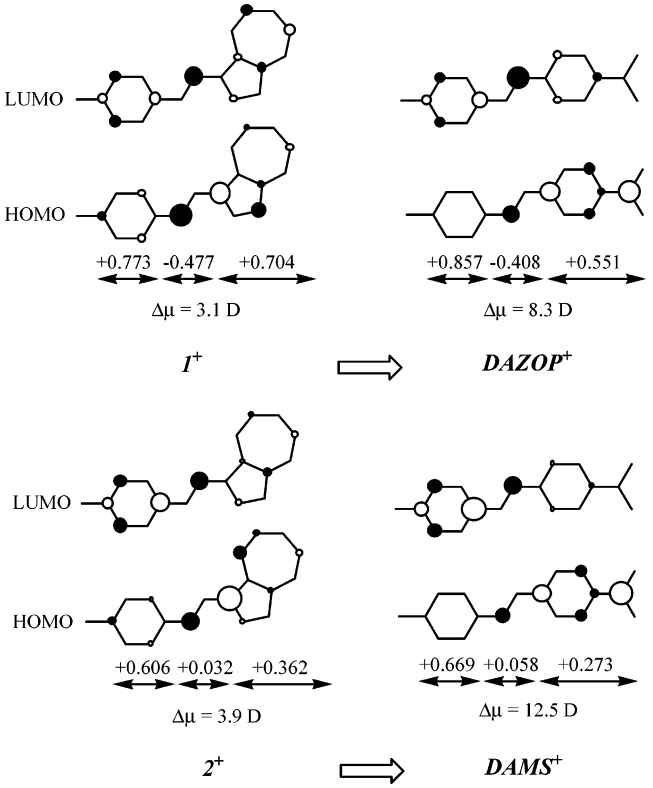

Figure 7. Frontier orbitals, with charge delocalization in the ground states (Mulliken charges) and excited states ($\Delta\mu$) for **1**$^+$ and **2**$^+$, versus those of their stilbazolium DAZOP$^+$ and DAMS$^+$ analogues.

related to the energy of the transition (E), its oscillator strength (f), and the difference between the ground- and excited-state dipole moments ($\Delta\mu$). The examination of the β_0 values in Table 3 reveals that the NLO response of azulene derivatives is surprisingly reduced versus that of the stilbazolium analogues. This fact strongly disagrees with the traditional idea that increasing the conjugation length and strength of donor acceptor groups eventually leads to β enhancement.

However, in the early 1990s, and in striking contrast to the previous approaches, Marder et al. proposed that, for a given bridge, there is an optimal combination of donor and acceptor strength which maximizes β.[61] Beyond this point, increasing the strength of the substituents leads to β attenuation. This deleterious effect occurs because the degree of mixing between the two canonical resonance forms (Scheme 3) is such that almost half of the charge available is transferred from the donor to the acceptor in both the ground and excited states, thus reducing $\Delta\mu$ (eq 1), and hence the β value.

To test this possibility for the present azulene derivatives, INDO calculations have been performed to evaluate the charge delocalization in the ground state in relation to $\Delta\mu$. The results are presented in Figure 7. The data reveal that the positive charge is mainly located on the pyridinium moiety of the stilbazolium derivatives, as indicated by the Mulliken populations. By contrast, it is more delocalized over the entire molecular structure in the related azulene chromophores, which leads to a reduced charge-transfer character in

(58) Olbrechts, G.; Wotsyn, K.; Clays, K.; Persoons, A.; Kang, S. H.; Kim, K. *Chem. Phys. Lett.* **1999**, *308*, 173.
(59) Uyeda, H. T.; Zhao, Y.; Wotsyn, K.; Asselberghs, I.; Clays, K.; Persoons, A.; Therien, M. J. *J. Am. Chem. Soc.* **2002**, *124*, 13806.
(60) (a) Oudar, J. L.; Chemla, J. *J. Chem. Phys.* **1977**, *66*, 2664. (b) Oudar, J. L. *J. Chem. Phys.* **1977**, *67*, 446.
(61) Marder, S. R.; Beratan, D. N.; Cheng, L. T. *Science* **1991**, *252*, 103.

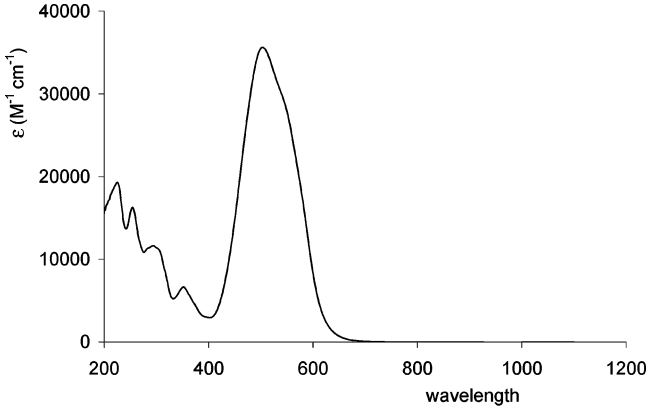

Figure 8. Electronic spectrum of $\mathbf{1}^+PF_6^-$ recorded in acetonitrile.

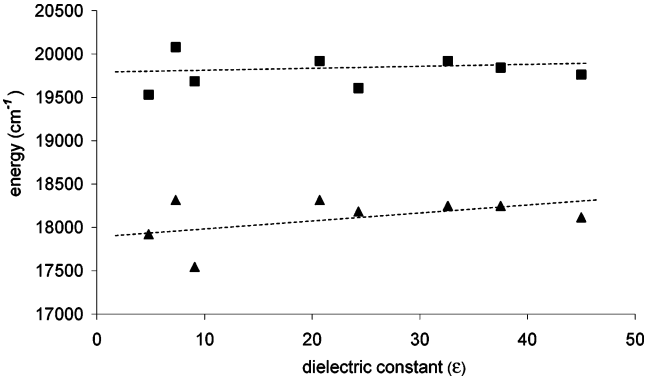

Figure 9. Comparison of the solvatochromic shift for the low-lying intense transition of $\mathbf{1}^+PF_6^-$ (squares) and DAZOP$^+PF_6^-$ (triangles).

the electron transition, and therefore to a reduced $\Delta\mu$, from 8−12 to 3−4 D. This effect is also suggested by the description of HOMO → LUMO excitation, which provides the dominant contribution to the NLO response in this series of chromophores. In Figure 7, the data clearly indicate a reduced push−pull character exhibited by the HOMO → LUMO excitation for the azulene derivatives. The reduction of $\Delta\mu$, which arises from an extremely efficient donor strength, completely agrees with the suggestion that the azulene substituent is located beyond the point which maximizes the hyperpolarizability in these pyridinium-based chromophores.

To find experimental support for this analysis, the solvatochromic properties have been investigated. $\mathbf{1}^+$, $\mathbf{2}^+$, and $\mathbf{3}^+$ all exhibit electronic spectra dominated by an intense band located at 503 nm (ϵ = 35600 M^{-1} cm^{-1}), 477 nm (ϵ = 43300 M^{-1} cm^{-1}), and 501 nm (ϵ = 23600 M^{-1} cm^{-1}), respectively. These low-lying bands, which are responsible for the NLO response of push−pull organic chromophores in the two-level approach (eq 1), are usually subjected to solvatochromism, a property related to the change in dipole moment occurring upon electron excitations. Although experimental estimation of $\Delta\mu$ by mean of solvatochromic shifts may not be fully reliable in some cases,[62] solvatochromism is generally strongly indicative of large $\Delta\mu$ values. This behavior is exemplified in the case of $\mathbf{1}^+$, for which the experimental β is the more significantly reduced (β_{DAZOP^+} = 154 → $\beta_{\mathbf{1}^+}$ = 67). The UV−vis spectrum of $\mathbf{1}^+PF_6^-$ recorded in MeCN is shown in Figure 8. The energies at the absorption maxima recorded in various solvents are shown in Figure 9, versus the dielectric constant in various media. The data are compared to those of DAZOP$^+PF_6^-$. The slopes of both curves (6.91 and 1.83 for DAZOP$^+$ and $\mathbf{1}^+$, respectively) may tentatively be used for providing a quantification of the solvatochromic properties, and may therefore allow an indirect measure of $\Delta\mu$. Within this approximation, the reduction of $\Delta\mu$ seems to be an important parameter to account for the β reduction.

This analysis leads to the suggestion that an alternative for azulene-based chromophores might be to envision their application in cubic nonlinear optics, where the π-electron polarizability certainly has to be important, but the push−pull character is not a prerequisite. Furthermore, Marder has suggested that the best strategy to optimize γ could be to decrease the change in dipole moment ($\Delta\mu$) occurring upon electron excitation.[9a] Along this line the present derivatives may offer additional interest. To provide more evidence for potential cubic NLO capabilities, a calculation has been conducted using the finite field (FF) procedure available with MOPAC. In this approach, γ is obtained as the numerical partial derivative of the energy (W) with respect to the electric field (E), evaluated at zero field, according to the following equation:

$$\gamma = -\left(\frac{\partial^4 W}{\partial E_i \partial E_j \partial E_k \partial E_l}\right)_{E=0}$$

Within this approach, the averaged γ is written as[63]

$$\gamma = 1/5(\gamma_{xxxx} + \gamma_{yyyy} + \gamma_{zzzz} + 2\gamma_{xxyy} + 2\gamma_{xxzz} + 2\gamma_{yyzz})$$

On the basis of this convention, the averaged γ values are equal to 43.9 × 10^{-36}, 30.7 × 10^{-36}, 8.4 × 10^{-36}, and 5.0 × 10^{-36} esu for $\mathbf{1}^+$, $\mathbf{2}^+$, DAZOP$^+$, and DAMS$^+$, respectively. Although these data result from a quick computational approach and, hence, should be used with caution, they tend to confirm that azulene-based cations with highly delocalized charge in the ground state could be envisioned as alternative materials with appealing cubic NLO response. On the basis of the spectral characteristics for these materials (a charge-transfer absorption band in the visible, yet transparency in the infrared), they offer potential for eye and sensor protection through nonlinear absorption in the visible, and for all-optical switching through the optical Kerr effect in the infrared. In this respect, they could attract some interest for the design of new organic materials for third-order optical nonlinearities.[64−66]

(62) See, for example: (a) Alain, V.; Rédoglia, S.; Blanchard-Desce, M.; Lebus, S.; Lukaszuk, K.; Wortmann, R. Gubler, U.; Bosshard, C.; Günter, P. *Chem. Phys.* **1999**, *245*, 51. (b) Blanchard-Desce, M.; Alain, V.; Midrier, L.; Wortmann, R. Lebus, S.; Glania, C.; Kramer, P.; Foert, A.; Muller, J.; Barzoukas, M. *J. Photochem. Photobiol., A* **1997**, *195*, 115.

(63) Nalwa, H. S. In ref 2b, p 515.

(64) For a review on cubic NLO properties, see: Stegeman, G. I. In ref 2b, p 799.

(65) For reviews on cubic NLO responses in organic molecules, see: (a) Nalwa, H. S. In ref 2b, p 611. (b) Brédas, J. L.; Adant, C.; Tackx, P.; Persoons, A. *Chem. Rev.* **1994**, *94*, 243.

(66) For an example of push−pull chromophores with large cubic NLO properties, see: Marder, S.; Torrulellas, W. E.; Blanchard-Desce, M.; Ricci, V.; Stegeman, G. I.; Gilmour, S.; Brédas, J. L.; Li, J.; Bublitz, G. U.; Boxer, S. G. *Science* **1997**, *276*, 1233.

Conclusion

The azulen-1-yl substituent exhibits an electron donor efficiency stronger than that of the well-known (dimethylamino)phenyl substituent, which has previously been used in the design of widely used chromophores, such as $DAMS^+$ or DR1.[67] Several pyridinium-based cations built up from this strong donor have been reported. They exhibit a tendency for crystallization into centrosymmetric space groups, and therefore, most of them are SHG silent. Nevertheless, alternative approaches have been reported in the literature to engineer these types of push−pull cations, into a noncentrosymmetric solid-state environment, for instance by insertion and intercalation chemistry.[68] Along this line, they could offer potential interest.

At the molecular level, these azulene derivatives exhibit sizable NLO responses, however with a tendency for β reduction, versus those of the (dimethylamino)-phenyl-based stilbazolium analogues. A set of structural data (bond lengths), spectroscopic properties (solvatochromism), and computational electronic features (Mulliken charges and $\Delta\mu$) were used to find a rationale for this behavior. Within a two-level model, the data suggest that the "charge-separated" canonical form is strongly involved in the ground states of these chromophores. This analysis leads to the idea that the electron donation strength of azulene may be beyond the point which maximizes the quadratic NLO response. By contrast, we point out that substituted azulene could attract additional interest in cubic nonlinear optics, and could therefore deserve further investigations in the future.

Acknowledgment. This research was supported through a European Community Marie Curie Fellowship. We thank Professor Keitaro Nakatani (PPSM, ENS Cachan, France) for the powder SHG measurements, Dr. Christine Lepetit (LCC, Toulouse) for her assistance in ZINDO calculations, and Ms. Sandra Parres (LCC, Toulouse) for 2D NMR measurements.

Supporting Information Available: Crystallographic data in CIF and PDF formats. This material is available free of charge via the Internet at http://pubs.acs.org.

CM0492989

(67) See, for example: (a) Izawa, K.; Okamaoto, N.; Sugihara, O. *Jpn. J. Appl. Phys.* **1993**, *32*, 807. (b) Choi, D. H.; Park, J. H.; Rhee, T. H.; Kim, N.; Lee, S. D. *Chem. Mater.* **1998**, *10*, 705. (c) Jiang, H.; Kakkar, A. K. *Macromolecules* **1998**, *31*, 2501.

(68) Bénard, S.; Yu, P.; Audière, J. P.; Rivière, E.; Clément, R.; Guilhem, J.; Tchertanov, L.; Nakatani, K. *J. Am. Chem. Soc.* **2000**, *122*, 9444.